A&A 415, 609–616 (2004)
DOI: 10.1051/0004-6361:20034623

Astronomy & Astrophysics

Hα variability of the recurrent nova T Coronae Borealis⋆

V. Stanishev[1,⋆⋆], R. Zamanov[2], N. Tomov[3], and P. Marziani[4]

[1] Institute of Astronomy, Bulgarian Academy of Sciences, 72 Tsarigradsko Shouse Blvd., 1784 Sofia, Bulgaria
[2] Astrophysics Research Institute, Liverpool John Moores University, Twelve Quays House, Egerton Wharf, Birkenhead CH41 1LD, UK
[3] Institute of Astronomy and Isaac Newton Institute of Chile – Bulgarian Branch, National Astronomical Observatory Rozhen, PO Box 136, 4700 Smolyan, Bulgaria
[4] INAF, Osservatorio Astronomico di Padova, Vicolo dell'Osservatorio 5, 35122 Padova, Italy

Received 25 July 2002 / Accepted 17 October 2003

Abstract. We analyze Hα observations of the recurrent nova T CrB obtained during the last decade. For the first time the Hα emission profile is analyzed after subtraction of the red giant contribution. Based on our new radial velocity measurements of the Hα emission line we estimate the component masses of T CrB. It is found that the hot component is most likely a massive white dwarf. We estimate the inclination and the component masses to be $i \simeq 67°$, $M_{\rm WD} \simeq 1.37 \pm 0.13\ M_\odot$ and $M_{\rm RG} \simeq 1.12 \pm 0.23\ M_\odot$, respectively. The radial velocity of the central dip in the Hα profile changes nearly in phase with that of the red giant's absorption lines. This suggests that the dip is most likely produced by absorption in the giant's wind.
Our observations cover an interval when the Hα and the U-band flux vary by a factor of ∼6, while the variability in B and V is much smaller. Based on our observations, and archival ultraviolet and optical data we show that the optical, ultraviolet and Hα fluxes strongly correlate. We argue that the presence of an accretion disc can account for most of the observed properties of T CrB.

Key words. accretion, accretion discs – stars: individual: T CrB – stars: novae, cataclysmic variables – stars: binaries: symbiotic

1. Introduction

T Coronae Borealis is a well known recurrent nova with an orbital period of 227$^{\rm d}$.57 (Kenyon & Garcia 1986; Fekel et al. 2000). The system contains a M4.5 III giant (Murset & Schmid 1999), which fills its Roche lobe and transfers mass toward a hot component (HC). The optical spectrum of T CrB is dominated by the red giant (RG) with superimposed Balmer emission lines, which are thought to originate in an accretion disc (AD) around the HC (Selvelli et al. 1992, hereafter SCG). The high excitation He II λ4686 emission line is sometimes also visible (Iijima 1990). The Hα emission line is well visible all the time and shows variability with the orbital period as well as large variations on a time scale of years (Anupama & Prabhu 1991; Zamanov & Marti 2001). The photometric variability in the long wavelength range is dominated by the ellipsoidal variability of the RG (Shahbaz et al. 1997; Belczynski & Mikolajewska 1998; Yudin & Munari 1993). At short wavelengths T CrB shows strong flickering activity, with the same parameters as those of normal cataclysmic variables, in spite of the large difference in the size of the AD (Zamanov & Bruch 1998). Apart from the recurrent nova outbursts, T CrB shows other periods of enhanced luminosity. The amplitude of these variations increases toward the shorter wavelengths and reaches ∼2 mag in the U-band (Zamanov & Zamanova 1997; Hric et al. 1998). The equivalent width of the line Hα (EW(Hα)) also greatly increases and reaches ∼30−35 Å (Anupama & Prabhu 1991; Zamanov & Marti 2001). This activity is not well understood.

For more than 30 years the HC in T CrB has been considered as a main sequence star (Kraft 1958; Kenyon & Garcia 1986). Investigations over the last 10 years, however, suggest that the accreting object must be a white dwarf (WD). First, SCG analyzed long-term ultraviolet (UV) spectral observations of T CrB and concluded that the HC is a WD. Belczynski & Mikolajewska (1998) analyzed the ellipsoidal variability of the RG and suggested the presence of a WD. In a study of recurrent novae with giant secondaries, Anupama & Mikolajewska (1999) also found that the HCs in these systems are WDs embedded in the dense wind of the RG. Finally, Hachisu & Kato (2001) successfully modeled recurrent novae outbursts as thermonuclear runaway on a massive WD. However, no system parameters determination based on the radial velocities (RVs) of the two components has been published since Kraft (1958). Recently, Hric et al. (1998) re-analyzed the RVs of Kraft (1958) and concluded that the hot component in T CrB is a WD.

Send offprint requests to: V. Stanishev, e-mail: vall@astro.bas.bg
⋆ Based on observations obtained at Rozhen National Astronomical Observatory, Bulgaria.
⋆⋆ Now at Physics Department, Stockholm University.

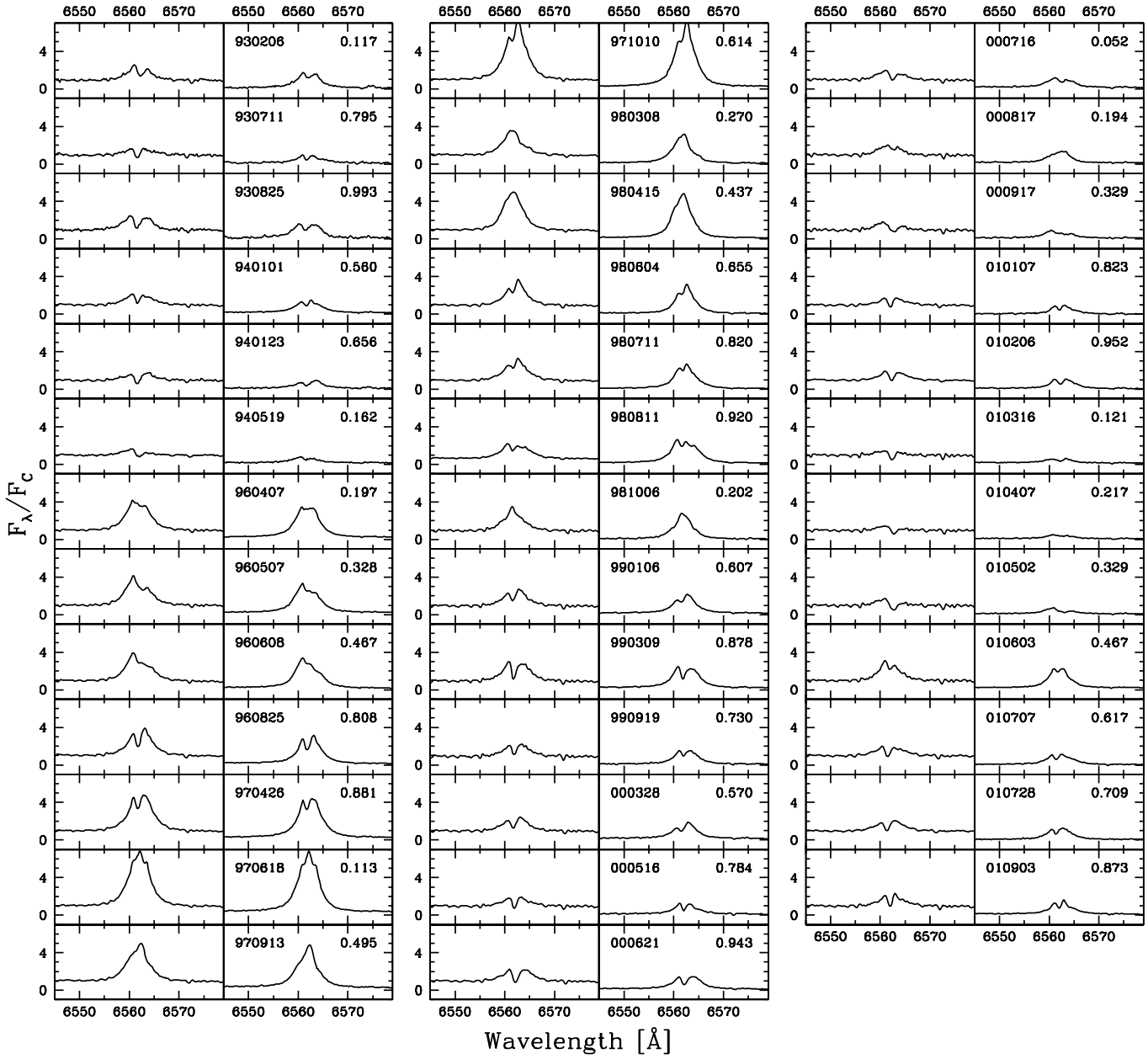

Fig. 1. Hα emission line profiles before (*left panels*) and after (*right panels*) the subtraction of the giant spectrum. The first number in each of the right panels shows the date of observations in YYMMDD format, and the second the orbital phase. Note that these phases were calculated with the orbital period of of Fekel et al. (2000), but the zero phase refers to the inferior conjunction of the RG.

However their analysis is still based on Kraft's seven measurements of the HC *RV*.

In this paper we present an analysis of spectral Hα and photoelectric *UBV* observations of T CrB obtained during the last decade. This is the first investigation of this object where the RG contribution is subtracted and the "cleaned" Hα profile is measured. Based on our Hα radial velocity measurements we obtain a new orbital solution. We also discuss the long-term variability of T CrB.

2. Observations and spectra processing

The star T CrB was observed during 64 nights between February 1993 and September 2001 with the Coudé spectrograph of the 2.0 m RCC telescope of the Bulgarian National Astronomical Observatory "Rozhen". The spectra cover ~100 Å or ~200 Å around Hα, with resolution of ~0.2 Å pixel^{-1}. In some nights we have also obtained spectra covering the He II λ4686 emission line. Usually 2 or 3 exposures, of 15−20 min each, were taken to improve the sensitivity and to avoid problems with cosmic ray hits. The spectra were reduced in the standard way including bias removal, flat-field correction, wavelength calibration and correction for the Earth's motion. The spectra obtained within each observational season (with a typical duration of 2−4 days) were averaged to improve the signal-to-noise ratio. 38 mean Hα spectra were obtained. They are plotted in the left panels of Fig. 1. We have also obtained new photoelectric *UBV* observations with

the 60 cm telescope at Rozhen Observatory (Zamanov et al. 2004, in preparation).

The main source of the continuum around Hα is the RG and the contribution of the HC is rather small, of the order of 5−15%. Because of this and since the Hα emission line is usually weak, the profile is strongly affected by the absorption lines of the RG. Therefore, to measure the *RV*s of the Hα emission line accurately one should first subtract the spectrum of the giant. To do this we used the following procedure. The M4 III star HD 134807 (Buscombe 1999) was observed with the same instrumental setup as T CrB and served as a template. The template was continuum-normalized and shifted to zero *RV*. Once Hα was masked, the *RV*s of the giant were obtained by convolving the T CrB spectra with the template (Tonry & Davis 1979). The template was then shifted to the *RV* of each spectrum, multiplied by a number f between 0 and 1 and subtracted from the T CrB spectra. f was chosen to minimize the scatter of the residuals. The width of the absorption lines in the spectra of both T CrB and the template is dominated by the spectral resolution rather than the rotational broadening. As a result the absorption lines have almost equal widths; however, in some cases the line widths are different. In those cases the average absorption line widths in the template and T CrB spectra were estimated by an autocorrelation function. Before the subtraction, the template or the spectrum was broadened by convolving it with a Gaussian to equalize the line widths. The "cleaned" Hα emission line profiles and the factors f used are shown in the right panels of Fig. 1 and in Table 1, respectively.

3. Radial velocities

The radial velocities of the Hα emission line were measured by fitting the line wings with a Gaussian function. We fitted only the outer parts of the line which are not contaminated by the central asymmetry/dip. Figure 1 shows that even after subtraction of the giant's spectrum the Hα line is double-peaked. When possible, the *RV* of the dip was also measured. A simple fitting with two Gaussian functions was used – one broad with a positive amplitude for the emission line and another narrow with a negative amplitude for the dip. Figure 2 shows the *RV*s of the giant, Hα emission line and the dip folded with the ephemeris of Fekel et al. (2000) T_0 = JD 2 447 918.62 + 227$^{\rm d}$.5687 E. The *RV*s were fitted with the function $V_{\rm r} = \gamma + K\cos[2\pi(\phi - \phi_0)]$ and the obtained parameters are given in Table 2.

The *RV* of the giant follows the ephemeris of Fekel et al. (2000) very well. The *RV* of the Hα wings changes in antiphase with that of the giant. This suggests that the location of the emission is on the line connecting the two stars, on the side of the mass center which is opposite to the giant. Most likely, the region where Hα emission line is formed is centered close to the HC. The observed ellipsoidal variability (Shahbaz et al. 1997; Yudin & Munari 1993; Belczynski & Mikolajewska 1998) suggests that the giant fills its Roche lobe, which provides a possibility for mass flow through the inner Lagrangian point and an AD formation. In this case the most plausible assumption is that the bulk of the Hα flux is emitted by the outer part of the AD. There is also other indirect evidence for the presence of an AD in this system (SCG; Anupama & Mikolajewska 1999; Hachusu & Kato 2001). Since the AD orbits around the mass center of the system together with the HC, the *RV*s of the emission line wings are likely to trace the motion of the HC. We will then use the radial velocity curves to estimate the component masses. Note, however, the small difference in the γ velocity of the HC and RG, and that ϕ_0 of the HC *RV*s is not exactly 0.5. This is likely to be a result of the presence of additional emission components which most

Table 1. The equivalent width *EW* and flux of the Hα line, its equivalent width after the giant spectrum subtraction *EW*(−*gM*), the factors f, and the radial velocity data of the HC, RG and central dip. The accuracy of the measurement is ∼10% in *EW* (mainly due to the uncertainty of the continuum placement), ∼20–40% in the flux (continuum placement and uncertainty of the continuum flux around Hα) and *EW*(−*gM*) (uncertainty of f) and ∼10–15 km s^{-1} in the radial velocities.

HJD–	*EW*	flux[a]	*EW*(−*gM*)	f	*RV*s [km s^{-1}]		
2 400 000	[Å]		[Å]		HC	RG	dip
49 026.12	7.5	4.4	63.8	0.86	–35.6	–7.6	–31.2
49 180.59	3.5	2.6	23.7	0.86	–9.8	–56.0	–49.2
49 225.45	8.4	4.6	69.6	0.86	–76.6	–44.0	–55.4
49 354.66	6.4	3.9	38.3	0.81	–41.1	–36.6	–55.4
49 376.55	4.0	2.8	31.7	0.86	–41.9	–50.0	–47.1
49 491.52	2.5	1.6	17.6	0.81	–79.5	–25.5	–77.9
50 182.16	17.9	12.4	66.7	0.72	–52.8	–5.3	...
50 211.95	15.5	10.9	65.0	0.74	–46.1	–4.5	...
50 243.60	15.0	9.2	76.6	0.79	–43.7	–27.1	...
50 321.36	14.6	10.4	72.8	0.82	–19.0	–55.3	–42.3
50 565.46	22.3	13.9	78.0	0.71	–23.1	–44.9	–44.2
50 618.35	29.6	17.3	75.0	0.60	–42.8	–14.1	...
50 705.24	20.0	12.0	55.0	0.66	–49.2	–30.6	...
50 732.20	31.3	19.9	127.1	0.73	–34.4	–42.6	...
50 881.48	12.8	9.4	124.3	0.89	–53.6	–11.2	...
50 919.48	19.9	12.4	143.3	0.86	–54.8	–22.9	...
50 969.31	12.2	8.3	95.7	0.91	–5.7	–48.7	–50.4
51 006.63	12.7	9.0	116.3	0.90	–22.9	–57.6	–44.9
51 029.62	14.1	8.4	77.4	0.82	–25.7	–48.8	–52.4
51 093.75	12.6	8.6	136.6	0.91	–47.3	–3.6	...
51 185.74	9.3	5.8	50.5	0.81	–20.4	–41.5	–55.8
51 247.46	12.2	7.7	46.8	0.75	–19.4	–45.3	–37.5
51 441.31	7.9	5.9	69.4	0.89	–23.4	–53.0	–33.2
51 632.55	7.6	4.6	40.4	0.81	–39.2	–38.9	–55.5
51 681.32	4.8	3.6	39.9	0.87	–24.4	–50.1	–34.1
51 717.38	7.3	4.2	46.8	0.84	–17.2	–31.4	–25.7
51 742.31	4.6	2.6	30.1	0.82	–43.4	–17.9	–16.1
51 774.62	5.7	3.9	31.8	0.83	–52.8	–10.1	...
51 805.27	3.1	2.2	27.8	0.86	–62.6	–14.5	...
51 917.64	3.1	2.2	98.7	0.96	4.1	–33.2	–33.8
51 947.06	4.7	2.7	44.3	0.89	6.5	–13.0	–23.7
51 985.47	0.8	0.5	11.2	0.81	–55.0	–8.4	–33.5
52 007.37	0.8	0.6	15.9	0.88	–57.7	6.6	–23.8
52 032.83	1.0	0.7	24.5	0.88	–53.9	–4.7	–6.9
52 064.34	9.3	5.6	42.3	0.76	–36.2	–14.9	–46.7
52 098.30	5.3	3.4	91.4	0.94	–33.6	–48.6	–60.4
52 119.44	5.6	4.2	98.9	0.92	–39.4	–67.1	–61.5
52 156.68	6.0	3.8	44.6	0.86	–6.5	–32.3	–37.7

[a] In units 10^{-12} erg cm^{-2} s^{-1}.

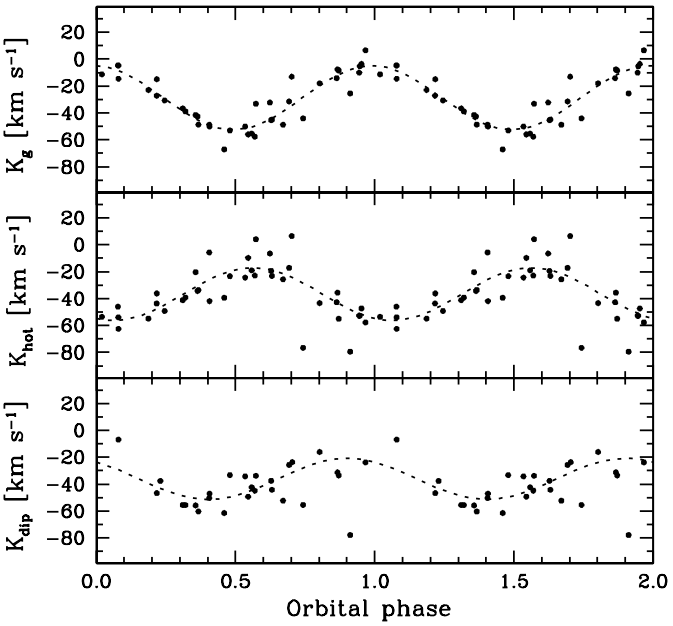

Fig. 2. The *RV*s of the giant, HC and the dip folded with the ephemeris of Fekel et al. (2000). The best fits are shown with dotted lines.

Table 2. The fit parameters to the Hα *RV* data.

	Red giant	Hot component	Central dip
γ [km s^{-1}]	–28.7 (1.4)	–36.7 (1.6)	–36.1 (2.3)
K [km s^{-1}]	23.7 (1.8)	19.5 (2.1)	15.2 (3.0)
ϕ_0	–0.009 (0.013)	0.563 (0.019)	–0.10 (0.03)
σ [km s^{-1}]	8.2	9.0	10.0

probably arise in the ionized parts of the giant's wind. Such emission components can be easily seen in Fig. 1 (the panels for 960608, 970618 and 980811).

If the double-peaked shape of Hα is a result of emission from an AD seen under moderate-to-high inclination, then the *RV* of the central dip should be in phase with that of the line wings. Figure 2 shows that the *RV* of the dip is modulated with the orbital period but follows more closely that of the giant, which argues against the AD origin. The central dip in the emission profiles of the symbiotic stars is thought to originate mainly in the giant's wind. In the symbiotic star EG And the *RV* of the dip also changes in phase with that of the giant (Munari 1993). Thus, the central dip in the Hα emission profile of T CrB originates most probably in the giant's wind.

4. Orbital solution

Having the *RV* amplitudes of the two components we can estimate their masses. The velocity amplitude of the giant in T CrB was accurately determined by Kenyon & Garcia (1986) – $K_{\rm RG} = 23.32 \pm 0.16$ km s^{-1} and was also recently revised to $K_{\rm RG} = 23.89 \pm 0.17$ km s^{-1} by Fekel et al. (2000). Our giant's velocity data are in full agreement with the results of these authors. But since our measurements are noisier, they lead to larger uncertainty of $K_{\rm RG}$. Thus, for determination of the system's parameters we prefer to use $K_{\rm RG}$ of Fekel et al. (2000). Assuming a zero eccentricity we obtain the following parameters: $M_{\rm HC} \sin^3 i = 1.06 \pm 0.10\ M_\odot$ and $M_{\rm RG} \sin^3 i = 0.87 \pm 0.18\ M_\odot$.

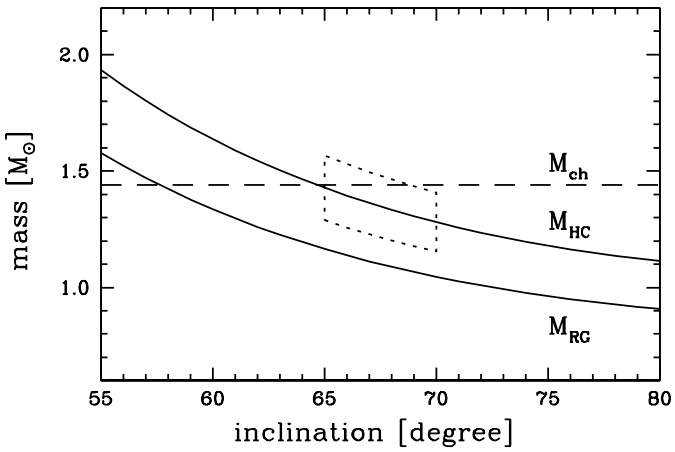

Fig. 3. The masses of the components of T CrB as a function of the inclination. The dotted curve shows the most likely position of the HC and the $i - mass$ space.

The masses of the two components as a function of the system inclination are shown in Fig. 3. Our HC velocities allow solutions with $M_{\rm HC}$ below the Chandrasekhar limit when the inclination is $i \geq 65°$. To obtain a more precise estimation of the masses a tighter constraint on the inclination is needed. The HC contributes little in the visible wavelengths but it gives almost the whole UV flux. Therefore, if the HC was eclipsed this would be best observed in the UV. The UV data, however, does not show any hint of eclipse (SCG) and it can provide an upper limit. We assume that the giant fills its Roche lobe. We have then numerically calculated the projection of the RG in the orbital plane at zero phase for several values of i between 60° and 80°, and component mass ratio $q = M_{\rm RG}/M_{\rm HC} = K_{\rm HC}/K_{\rm RG} = 0.82 \pm 0.10$. We found that the center of the HC is not eclipsed when $i \leq 70°$. The upper limit depends also on the size of the UV emitting region. Its size, however, should be very small compared to the radius of the HC's Roche lobe because the most likely UV emitting region is the WD and the inner part of the AD (SCG). Thus, we conclude that the upper limit of the inclination is ~70°. The dotted lines in Fig. 3 mark the limits of the inclination and $\pm 1\sigma$ of the HC mass. Recently, Hachisu & Kato (2001) have modeled the outburst light curve of T CrB and obtained the WD mass $M_{\rm WD} \simeq 1.37 \pm 0.01\ M_\odot$. In terms of our orbital solution this corresponds to $i \simeq 67°$ and for this inclination we have $M_{\rm WD} \simeq 1.37 \pm 0.13\ M_\odot$ and $M_{\rm RG} \simeq 1.12 \pm 0.23\ M_\odot$.

5. Long-term variability

In Fig. 4 we show our observations of T CrB along with those published. Figure 4a shows our EW(Hα) measurements (dots) and those of Anupama & Prabhu (1991) (open circles). Figures 4b and c show the total UV flux between 1250 and 3200 Å ($F_{\rm UV}$; taken from SCG) and EW(Hα) measured from our spectra after the subtraction of the RG contribution (hereafter EW(H$\alpha - gM$)), respectively. In the photometry

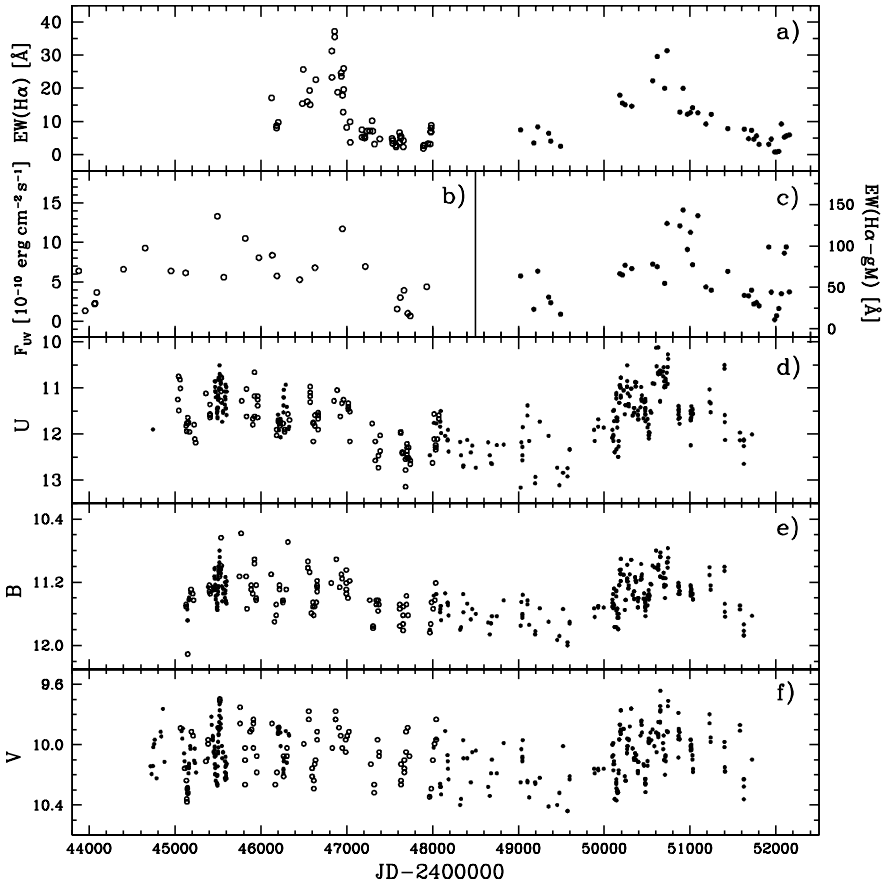

Fig. 4. a) Hα equivalent width; **b)** total UV flux between 1250 and 3200 Å; **c)** Hα equivalent width after the subtraction of the RG spectrum; **d)** *U* magnitudes, **e)** *B* magnitudes and **f)** *V* magnitudes. See text for the sources of the different quantities.

panels (Figs. 4d–f) the dots show the standard *UBV* magnitudes (Raikova & Antov 1986; Lines et al. 1988; Hric et al. 1998; Sherrington & Jameson 1983; Zamanov & Zamanova 1997; our new data) and the open circles the instrumental ones (Oskanian 1983; Luthardt 1992). The data of Luthardt were presented only in graphical form as a difference between T CrB and the comparison star which was not specified. We estimated the magnitudes of T CrB from the figure of Luthardt (1992) in the following way. On the computer screen we pointed with the cursor on each data point and read its coordinates. These "computer screen" coordinates were converted to Julian Dates and magnitudes by applying the necessary transformations. Then, the data were shifted to the scale of the standard magnitudes by using the intervals when they overlap with the *UBV* observations. We have also obtained an estimation of the Hα flux by using the measured EW(Hα) and the published *R*-band magnitudes. We assume that the *R*-band flux represents the continuum flux at the position of Hα and that the variations in *R* are entirely due to the ellipsoidal variability. We fitted the *R* data of Mikolajewski et al. (1997) and Hric et al. (1998) with a function consisting of three sines with periods of $P_{\rm orb}$, $P_{\rm orb}/2$ and $P_{\rm orb}/3$. With the coefficients obtained we have calculated the *R* magnitudes at the moments of the spectral observations. Then, Bessell's (1979) calibration of the *R*-band was used to calculate the Hα flux. Because the Hα flux variations repeat very closely those of EW(Hα), the Hα flux is given only in Table 1 (only for our spectra). We note that the assumption that the *R*-band flux represents the flux in the continuum around Hα introduces the largest uncertainty in the calculated Hα flux. The reason is that the *R* filter covers several strong molecular bands, and is placed where the flux in the RG spectrum increases strongly toward the long wavelengths.

As seen from Fig. 4 our observations cover an interval when both the photometric data and EW(Hα) vary greatly. The long-term variability has amplitude ∼2.0, 1.0 and 0.3 mag in *U*, *B* and *V* bands, respectively. EW(Hα) increased from ∼5 Å to ∼30 Å. EW(Hα−*gM*) also increased, but its maximum is delayed with respect to the maximum of EW(Hα) and appears at JD 2 450 950. It is seen from Figs. 4d and e that the maximum of EW(Hα−*gM*) coincides with the rapid decrease of the *U* and *B*-band fluxes. This might explain the observed peculiarity. It is also seen from Fig. 4 that most of the UV observations have been obtained when T CrB was in a high state. It is quite evident, however, that during the observations around JD 2 444 000 and JD 2 447 700 T CrB was in a low state. The average increase of $F_{\rm UV}$ is ∼3.3 and the corresponding increase of the *U*-band flux is ∼2.6 (∼1 mag).

Anupama & Mikolajewska (1999) noticed that the increase of EW(Hα) in the late 1980s correlated with the increase of UV and *U* fluxes. Our new observations also show similar behavior. To verify the strong visual impression for correlation of the data shown in Fig. 4 we performed a correlation analysis. The small number of UV observations required interpolation when calculating the correlations involving $F_{\rm UV}$. For the correlation between Hα and *U*-band fluxes we used yearly averaged values. (EW(Hα−*gM*) was not used here). The computed Pearson's correlation coefficient and Spearman's rank correlation coefficient are in all cases larger than 0.7 with the significance of the

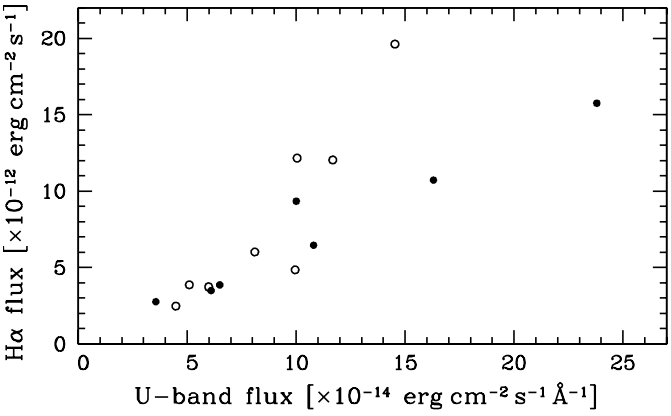

Fig. 5. The yearly averaged Hα flux vs. the U-band flux. Dots represent our data and open circles those of Anupama & Prabhu (1991).

correlation always higher than 99%. The correlation analysis confirmed that all the data in Fig. 4 are indeed strongly correlated. As an example we show Hα vs. U-band flux in Fig. 5. Our data and those of Anupama & Prabhu (1991) follow different tracks, but the correlation is apparent.

The correlated variations in the continuum can be also seen in Fig. 6 where we present the UV-optical-IR spectral energy distribution (SED) of T CrB in low and high states. The points are a compilation (average) from the photometric data of Shahbaz et al. (1997), Kamath & Ashok (1999), Yudin & Munari (1993), Munari et al. (1992), Hric et al. (1998), Mikolajewski et al. (1997), Zamanov & Zamanova (1997) and our measurements. A representative high-state UV spectrum of T CrB was obtained by averaging the low-resolution spectra taken by the International Ultraviolet Explorer (*IUE*) between JD 2 444 300 and JD 2 447 300 when the system was in high state. The rest of the *IUE* spectra were used to obtain the average low-state UV spectrum. All fluxes were corrected for interstellar reddening of $E_{B-V} = 0.15$ (Cassatella et al. 1982) using O'Donnell's (1994) interstellar extinction law and $R_V = 3.1$.

The data in Figs. 4b and 6 show that the bolometric luminosity of the hot component varies greatly on time scale of about 200 days, which is not a typical feature of objects whose activity is powered by thermonuclear runaways. Moreover, SCG demonstrated that the bolometric luminosity of the hot component is low ($\sim$100 $L_\odot$) compared to some other symbiotic systems whose activity is supposed to be due to hydrogen burning (e.g., AG Peg, AG Dra, Z And) and that even in the low state most of the hot component's light is emitted in the UV. All these characteristics suggest that the system is accretion powered and the hot component is most probably the innermost part of an optically thick accretion disc and/or the boundary layer between the disc and the WD's surface as was already proposed by SCG. This idea supports our previous assumption based on the behavior of the Hα radial velocity (Sect. 3) that the bulk of the energy of this line is probably emitted by the outer part of an AD.

According to the AD theory (e.g., Warner 1995), there exists a critical value $\dot{M}_{\rm cr}$ of the mass accretion rate $\dot{M}$, so that if $\dot{M} > \dot{M}_{\rm cr}$ the disc is in a steady state, being hot and optically thick with effective temperature $T_{\rm eff,hot} \propto \dot{M}^{1/4} M_{\rm WD}^{1/4} r^{-3/4}$ ($T_{\rm eff,hot} > 10^4$ K). Here r is the distance to the WD. If $\dot{M} < \dot{M}_{\rm cr}$ the disc is cool and optically thin with $T_{\rm eff,cool} \simeq 5{-}6 \times 10^3$ K. With the parameters of T CrB $\dot{M} \sim 10^{-8}\, M_\odot\, {\rm yr}^{-1}$ (SCG) and $M_{\rm WD} \simeq 1.37$, only the inner part of the disc with radius $\sim$1 $R_\odot$ is in the hot state, while the rest of the disc is cool. In the case of accretion at a high rate onto a very massive WD, as in T CrB, the temperature of the innermost part of the disc should be $\sim 1{-}2 \times 10^5$ K. It will thus emit mostly in the UV and can be the HC. In this case variations of $\dot{M}$ can easily account for its observed variability.

The symbiotic systems containing a hot compact object change their energy distribution appreciably during active phase because of the variation of the temperature of the compact object. Figure 6 shows that the UV energy distribution of T CrB tends not to vary during its transition from low to high states. SCG notice a correlation of the slope of the continuum with the total UV flux. However, using the values given in their Table 1, we found that the correlation, if any, is very weak. Thus, the modeling of the continuum requires nearly the same temperature of the hot component in low and high states. We tried to model the continuum of T CrB assuming the presence of an optically thick AD. The IR region was fitted with synthetic fluxes of a model spectrum of a red giant with $T_{\rm eff} = 3500$ K, $M = 1\ M_\odot$ (Hauschildt, private communication) and $R = 75\ R_\odot$, filling its Roche lobe. The UV and visual regions were fitted with an emission of an AD and gas environment. We adopted an electron temperature of 10 000 K according to SCG. Thus, the only free parameters are the mass accretion rate and the relative scaling between the three components.

To determine the nebular continuum, the ionization state of helium has to be known. The dominant state of ionization can be estimated from the ratio of the emission measures of the neutral and ionized helium based on the fluxes of some lines of He I and the He II λ4686 line. Since the electron temperature of 10 000 K is comparatively low we assumed that He I lines are determined only by recombination. Our observations of the He II λ4686 line show that most of the time this line was absent and only occasionally appeared very weak. The line was also not presented in the spectrum in July 1986, as can be seen in Fig. 2 of SCG. According to Iijima (1990) in the period 1981−1987 T CrB has had prominent emission lines of He I whereas its He II λ4686 line was only temporarily observed. In the spectra taken in Apr.–May 1997 during the recent high state, Anupama & Mikolajewska (1999) detected the He II λ4686 line, but it was by a factor of 2 weaker than the He I lines. At an electron temperature of 10 000 K and electron density of 10^6 cm^{-3} if the number of He^+ and He^{++} ions is the same, the intensity of the He II λ4686 line exceeds the intensities of the He I lines by one order of magnitude (e.g. Pottasch 1984). This was probably not the case during the period of Iijima's observations. Thus, we accepted the dominant helium ionization state He II in all occasions and assumed that the nebular continuum is mostly continuum emission of hydrogen and neutral helium. We adopted a helium abundance of 0.1 (Nussbaumer & Vogel 1989) and distance to the system of 1.3 kpc (Patterson 1984).

The result of the modeling is shown in Fig. 6. To determine the level of the UV continuum of T CrB is a complicated

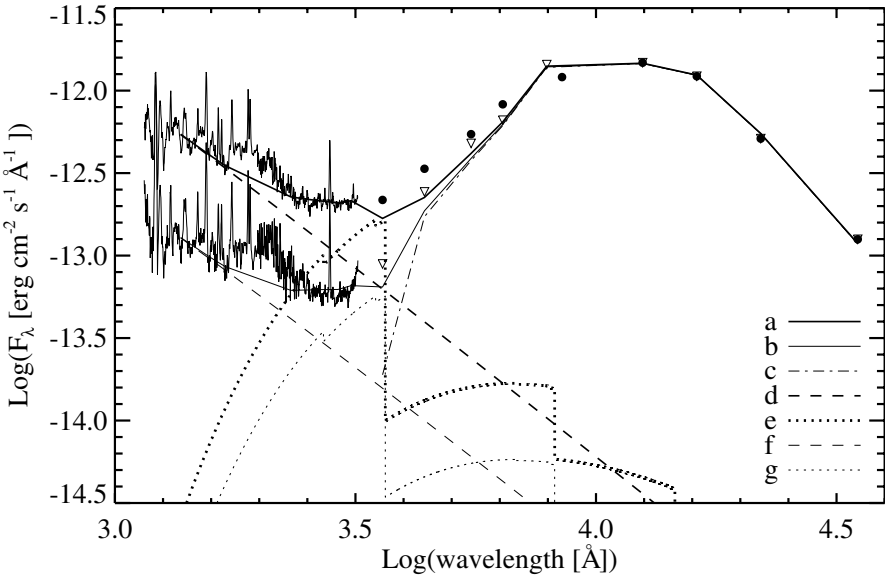

Fig. 6. UV-optical-IR energy distribution of T CrB. The representative UV spectra are related to its low and high states. The triangles and the filled dots indicate the photometric fluxes at low and high states, respectively. Lines **a)** and **b)** show the model spectrum of the system in high and low state, respectively. Line **c)** connects the synthetic fluxes of a red giant. Lines **d)** and **e)** indicate the continia of the accretion disc and the nebula in high state. Lines **f)** and **g)** show the same components for the low state.

task – the spectrum is dominated by humps caused by blended emission lines. We fitted the bottoms of the troughs between those humps. The largest discrepancies between the fit and the spectrum are in the short-wavelength region and around 2200 Å where the sensitivity of *IUE* is low. It is seen, however, that the shape of the fit to the UV spectrum in the two states is nearly the same. The observed optical fluxes in both states are systematically higher than the fit. This indicates the presence of component(s) which are not taken onto account in our model. This additional light might be due to density and temperature inhomogeneities in the outer disc or/and in the other nebular formations in the system.

The modeling gave an accretion rate of $4\times10^{-9}\ M_\odot\ \mathrm{yr}^{-1}$ for the low state and $3\times10^{-8}\ M_\odot\ \mathrm{yr}^{-1}$ for the high state in agreement with SCG. Note also that at these accretion rates the disc temperature exceeds 10^5 K. At such temperatures the scope of the UV continuum is nearly constant.

We obtained appreciable emission measures of 2.7×10^{59} cm^{-3} and 7.4×10^{59} cm^{-3} for the low and high states, determined from strong nebular UV and optical continuum. On the other hand the Balmer emission lines are weak (Hα exceeds the level of the continuum by a factor of not greater than 5−6). The symbiotic systems with an extended surrounding nebula (AG Dra, Z And) have prominent Balmer emission lines exceeding the continuum by a factor of up to 40−50, together with their intensive nebular continuous spectrum. In the case of T CrB the weakness of the Balmer emission lines can be understood if they are assumed to be formed in a gas medium with a great optical depth, which absorbs the dominant part of the photons. The optical depth is great when the column density of the emitting gas is high. Anupama & Mikolajewska (1999) came to the conclusion that the hot component of the symbiotic recurrent novae is most probably a white dwarf + accretion disc embedded in an optically thick envelope formed by the wind of the M giant secondary. This model provides high column density and contains an AD as well. So, the weak Balmer lines of T CrB can be qualitatively explained by the assumption of an origin in a binary system containing an AD. The investigation of the *RV* of the Hα line showed that the bulk of its energy is emitted by an area around the hot component – probably the outer part of an AD. This model is supported also by our suggestion for the explanation of the weak Balmer emission lines of T CrB. The modeling of T CrB's SED suggests that the UV spectrum appears flat mostly because of the strong nebular contribution. However, it is also possible that this is partly a result of seeing the AD at a relatively high inclination as suggested by SCG.

The evidence for an AD and high $\dot{M}$ provides good conditions for formation of intensive high-speed wind emerging from the innermost hot parts of the disc (see Mauche & Raymond 1997 for a discussion of disc wind in the case of cataclysmic variables). Consequently the nebular spectrum of the system may appear also in the winds of the disc and the cool giant in addition of the disc itself. Shore & Aufdenberg (1993) showed that the giant's wind is variable. Further evidence for this can be found in the variations of the central dip of the Hα emission line – most of the time the dip is well pronounced, but sometimes it is highly variable and is almost absent (Fig. 1).

If an AD is present in T CrB system, its activity may be a result of variation of the accretion rate $\dot{M}$. There are two ways to increase $\dot{M}$: (1) to increase the mass transfer rate $\dot{M}_{\rm tr}$ from the giant and (2) to increase temporarily the mass flow through the AD. The former may be a result of the magnetic activity of the giant as suggested by Soker (2002). The later mechanism corresponds to the outbursts observed in the dwarf novae and is related to the so-called disc instability. In the context of symbiotic stars the disc instability was studied by Duschl (1986), but assuming that the accreting object is an ∼1 $M_\odot$ main-sequence star rather than a WD. Briefly, in the disc instability model $\dot{M}_{\rm tr}$ is constant and less than $\dot{M}_{\rm cr}$, i.e. the disc is in the cool state most of the time. Outburst is observed when $\dot{M}$ (locally in the disc) increases above $\dot{M}_{\rm cr}$ and the AD rapidly approaches the hot state (for more details see Warner 1995). In both cases the disc luminosity increases because of the dependence of the temperature on the mass accretion rate: $T_{\rm eff,hot} \propto \dot{M}^{1/4}$.

6. Summary and conclusions

The radial velocities of the Hα emission line of the recurrent nova T CrB were precisely measured after subtraction of the red giant spectrum, thus obtaining the unbiased Hα profile. Based on our 38 new radial velocity measurements we obtain a new solution for the system parameters. The solution indicates that at a system inclination $i > 65°$ the mass of the hot component is below the Chandrasekhar limit and thus the hot component in T CrB is most likely a massive white dwarf. The most likely values of the system inclination and the component masses are $i \simeq 67°$, $M_{\rm WD} \simeq 1.37 \pm 0.13\ M_\odot$ and $M_{\rm RG} \simeq 1.12 \pm 0.23\ M_\odot$.

The radial velocity of the central dip of the Hα emission line profile changes almost in phase with that of the red giant. This suggests that the central dip originates from the giant's wind.

During our observations T CrB showed a period of activity when the system brightness increased by ∼2.0, 1.0 and 0.3 mag in U, B and V bands, respectively. The Hα equivalent width also increased by a factor of ∼6 reaching ∼30 Å and the line had a complex multi-component structure. The phasing of the modulation of Hα emission line radial velocity shows that the emitting region is gravitationally connected to the hot component of the system and most probably related to the outer part of an accretion disc. We argue that a number of other characteristics of T CrB are also in support of this supposition. The long-term variability is then assumed to be caused by variations of the mass accretion rate, possibly due to changes of the mass transfer rate from the companion or disc instability. This is also supported by our success in modeling the UV-optical-IR SED of T CrB with a three-component model: an optically thick accretion disc, a nebular continuum and a red giant. However, to construct a consistent picture and to understand the underlying physical processes in T CrB better, simultaneous UV and optical spectral observations during future active phases are needed. Space observatories offering simultaneous optical/UV spectroscopic capabilities like Kronos (Peterson et al. 2001) and WSO/UV (Wamsteker & Ponz 2001) would be a good solution.

References

Anupama, G. C., & Mikolajewska, J. 1999, A&A, 344, 177
Anupama, G. C., & Prabhu, T. P. 1991, MNRAS, 253, 605
Belczynski, K., & Mikolajewska, J. 1998, MNRAS, 296, 77
Bessell, M. S. 1979, PASP, 91, 589
Buscombe, W. 1999, 14th General Catalogue of MK Spectral Classification, Northwestern Univ., Evanston, Illinois ISBN 0-939160-12-9
Cassatella, A., Patriarchi, P., Selvelli, P. L., et al. 1982, in Third IUE European Conference (ESA-SP 176), 229
Duschl, W. J. 1986, A&A, 163, 61
Fekel, F. C., Joyce, R. R., Hinkle, K. H., & Skrutskie, M. F. 2000, AJ, 119, 1375
Hachusu, I., & Kato, M. 2001, ApJ, 558, 323
Hric, L., Petrik, K., Urban, Z., et al. 1998, A&A, 339, 449
Iijima, T. 1990, JAVSO, 19, 28
Kamath, U. S., & Ashok, N. M. 1999, A&ASS, 135, 199
Kenyon, S. J., & Garcia, M. R. 1986, AJ, 91, 125
Kraft, R. P. 1958, ApJ, 127, 620
Lines, H. C., Lines, R. D., & McFoul, T. G. 1988, AJ, 95, 1505
Luthardt, R. 1992, ASP Conf. Ser. 29, ed. N. Vogt, 375
Mauche, C. W., & Raymond, J. C. 1997, in Cosmic Winds and the Heloisphere, ed. J. R. Jokipii, C. P. Sonett, & M. S. Giampapa (Tucson: University of Arizona Press), 111
Mikolajewski, M., Tomov, T., & Kolev, D. 1997, IBVS, 4428
Munari, U. 1993, A&A, 273, 425
Munari, U., Yudin, B. F., Taranova, O. G., et al. 1992, A&AS, 93, 383
Murset, U., & Schmid, H. M. 1999, A&AS, 137, 473
Nussbaumer, H., & Vogel, M. 1989, A&A, 213, 137
O'Donnell, J. 1994, ApJ, 422, 158
Oskanian, A. V. 1983, IBVS, 2349
Patterson, J. 1984, ApJS, 54, 443
Peterson, B. M., & Kronos Science Team 2001, Amer. Astron. Soc. Meet., 199, 4507
Pottasch, S. R. 1984, Planetary Nebulae (Dordrecht: Reidel), 59
Raikova, D., & Antov, A. 1986, IBVS, 2960
Selvelli, P. L., Cassatella, A., & Gilmozzi, R. 1992, ApJ, 393, 298 (SCG)
Shore, S., & Aufdenberg, J. 1993, ApJ, 416, 355
Soker, N. 2002, MNRAS, 337, 1038
Shahbaz, T., Somers, M., Yudin, B., & Naylor, T. 1997, MNRAS, 288, 1027
Sherrington, M. R., & Jameson, R. F. 1983, MNRAS, 205, 265
Tonry, J., & Davis, M. 1979, AJ, 84, 1511
Wamsteker, W., & Ponz, J. D. 2001, AGM, 18, #JD404
Warner, B. 1995, Cataclysmic Variable Stars (Cambridge University Press)
Webbink, R. F. 1976, Nature, 262, 271
Yudin, B., & Munari, U. 1993, A&A, 270, 165
Zamanov, R., & Bruch, A. 1998, A&A, 338, 988
Zamanov, R., & Marti, J. 2001, IBVS, 5013, 1
Zamanov, R., & Zamanova, V. 1997, IBVS, 4461